CREEP EFFECTS ON TENSION PILES FOR THE DESIGN OF BUOYANT OFFSHORE STRUCTURES

J A Ramalho-Ortigão[1] and M F Randolph[2]

Federal University of Rio de Janeiro, Brasil[1]
Cambridge University, UK[2]

INTRODUCTION

During the past 10 years the petroleum industry has been considering the use of floating production systems for the development of deep water offshore oil fields. The rapidly increasing costs of the conventional jacket or gravity structures in deep waters (see Figure 1) have been a challenge for the design of unconventional solutions.

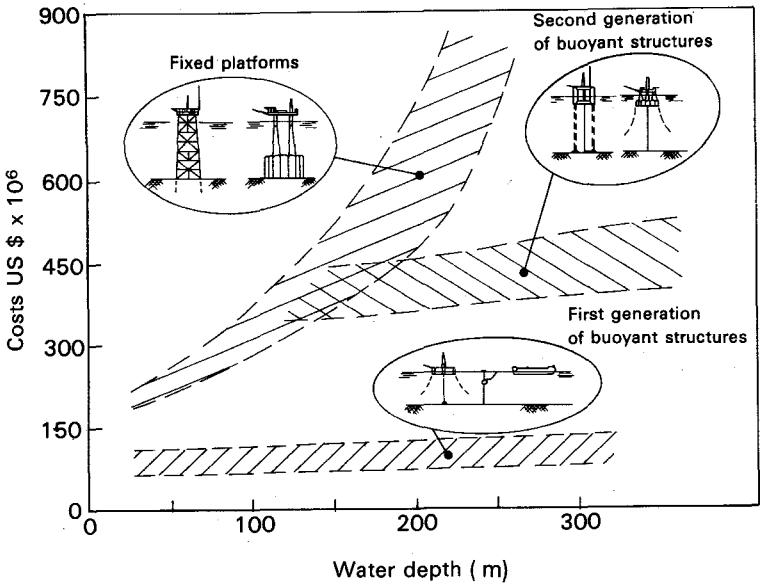

Figure 1 Cost Trends (apud Hamilton and Barrack, 1978)

A recent proposal, the Hutton tension leg platform, (Tetlow and Leece, 1982) is to be used in water 148 m deep in the North Sea. This platform is to be anchored by a system of four tethers, each transferring the tension load to a pile group consisting of eight driven cylindrical steel piles.

In Brasil, Hamilton and Barrack (1978) reported the use by Petrobras of a SEDCO 135D semi-submersible facility moored by a spread anchor system.

The design of tension piles to withstand the loads from such platform types poses a new challenge to geotechnical engineers, since most of the experience with both land and offshore piles has been in compression and only occasionally in tension.

As an attempt to develop a design tool for offshore tension loaded piles, this paper shows the application of a stress-transfer function incorporating creep to the analyses of two piles driven in clay. These piles were tested at different rates and creep was considered the main aspect which influenced the difference in their behaviour.

A BRIEF REVIEW OF FACTORS AFFECTING THE CAPACITY OF TENSION PILES

The design of piles in tension has been reviewed recently (eg. Gallagher et alii, 1980, St John, 1980, St John et alii, 1983) and from those studies the following points are quoted:

1. The key problem for the design of piles in tension is to avoid irrecoverable upward movements which will lead to a reduction in capacity.

2. Neglecting the suction at the base of the pile, the problem of the design of a tension pile reduces to evaluating its shaft behaviour. There is no evidence that the shaft behaviour in tension is different from that in compression, and so the design methods for the latter may be applied.

   The shaft capacity of a pile has been evaluated by an expression of the form:

$$Q_s = \int_0^{\ell} \tau_s \, f(z) \, dz$$

where

ℓ = length of the pile
$f(z)$ = outer perimeter of the pile as a function of its depth
$\tau_s(z)$ = the unit shaft friction as a function of depth

In sands the unit friction $\tau_s(z)$ can be evaluated as a function of the angle of friction between the interface soil-pile and the horizontal effective stress (eg. API RP2A). In clays the following methods have been applied.

(i) total stress method: the α method (eg. API RP2A, DNV, 1981)

(ii) effective stress methods: the β method (eg. Burland, 1973) and critical state methods (Kraft, 1982)

(iii) the λ method, which is a combination of (i) and (ii) (eg. Vijayvergiya and Focht, 1972).

The following factors have been reported to affect the shaft capacity of piles:

(i) length effect (pile flexibility);

(ii) cyclic loading and rate effects;

(iii) creep effects.

A comprehensive review of these problems can be found in St John et alii (1983). This paper, however, will further concentrate on the latter - the creep effects - and present the results of a study carried out to evaluate the behaviour of two piles in clay tested with different rates of tensile loading.

MODELLING TENSION PILES

A one dimensional model of the pile, similar to the one described by Kraft et alii (1982), was employed. This model has the advantage of being reasonably simple (avoiding the complications of a finite element analysis) but at the same time, with a little modification, allows the incorporation of a complex load transfer curve. The pile is modelled by a system of lumped masses interconnected by linear springs representing its axial stiffness. The pile-soil interface stress transfer curve is simulated by non-linear springs as shown in Figure 2.

A computer program, RATZ, incorporating this model has been written by Randolph (1982). The stress transfer curve is portrayed on Figure 3 and has already been described by St John et alii (1983). In the first part, soil and pile are treated as a continuum and the displacements around the pile are considered to be proportional to the pile diameter. At low stress levels soil pile interaction is simulated by a linear relationship which lasts until a yield shear stress occurs. Until shear stresses reach their peak value, a parabolic relationship is assumed between shear stress and normalised displacements against pile radius.

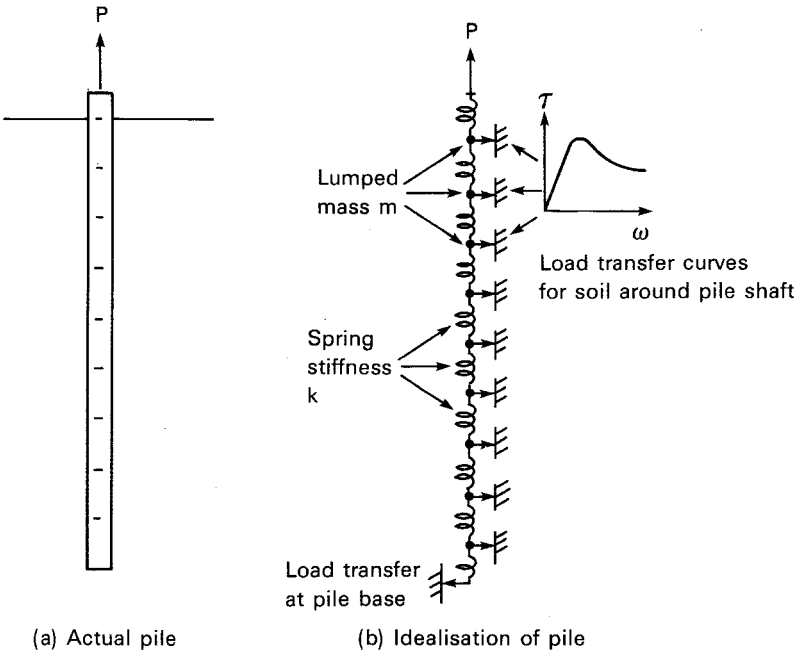

Figure 2 Idealisation of pile in load Transfer Analysis

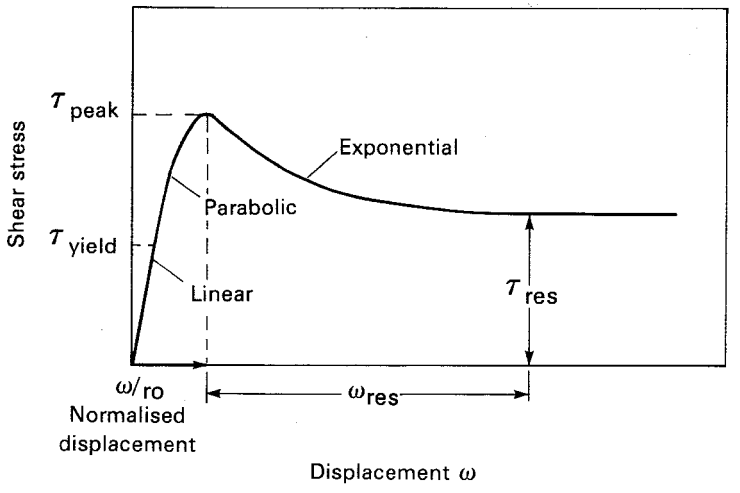

Figure 3 Load Transfer curve

The following parameters were chosen to describe the initial part of the curve up to peak:

k = slope of linear part of the curve = $d\tau/d(w/r_o)$
τ_y = yield shear stress, below which no degradation occurs
τ_{peak} = peak shear stress

A relationship between k and the shear modulus of the soil can be obtained. From the work of Randolph and Wroth (1978), k was found to be 20 to 30% of the soil shear modulus.

At peak, a discontinuity between soil and pile is assumed to occur and the displacements are no longer considered to be normalised. The value of shear stress then starts to fall with pile displacement until a residual value τ_{res} is reached. The shear stress degradation from peak value to residual, is assumed to follow an exponential law given by:

$$\tau_f = \tau_{peak} - 1.1(\tau_{peak} - \tau_{res})[(1 - \exp(-2.4\ (w_c/w_{res})]^{\zeta}$$

where
τ_f = current failure shear stress;
τ_{res} = residual failure shear stress;
w_c = current displacement;
w_{res} = additional displacement that provokes shear stress to fall from peak to residual value;
ζ = degradation parameter, responsible for the shape of the degradation curve.

Implementation of the effects of creep were achieved as shown on Figure 4. A strain controlled approach was employed by shifting the stress-displacement curve by an amount Δw which was obtained by an equation similar to the one proposed by Singh and Mitchell (1968):

Singh and Mitchell:

$$\Delta w = A \exp(\alpha\ \tau_c/\tau_f)\ (t_o/t)^m \Delta t \qquad \text{Equation 1}$$

Computer Model:

$$\Delta w = \beta \exp(\alpha\ \tau_c/\tau_f)\ (\Delta t/t)^m (w_c - w_o) \qquad \text{Equation 2}$$

where

A, α, m, β = creep parameters
w_c = the current displacement
w_o = a reference displacement after the pile has been allowed to rebound from to zero shear stress
t_o = reference time
t = time
Δt = time increment

This equation is written in a non-dimensional form, where the reference time t_o has effectively been replaced by the time increment in the explicit time formulation of the program

RATZ. The factor $(w_c - w_o)$ is included to make the parameter β dimensionless.

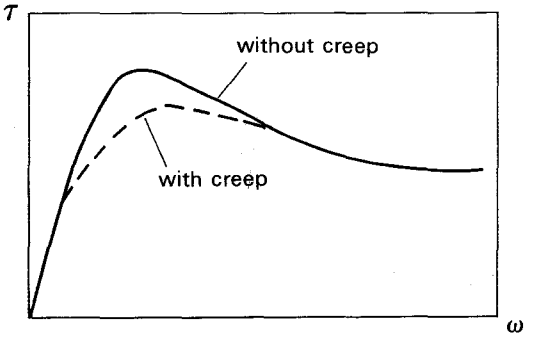

(a) Effect of soil creep

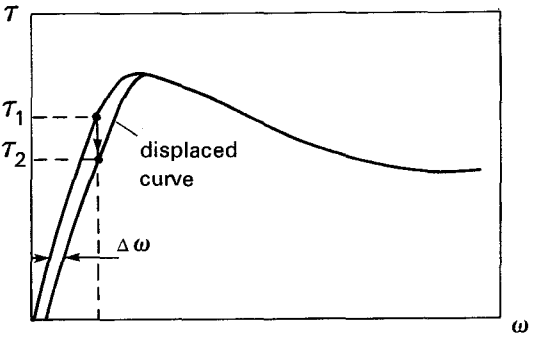

(b) Displacement of load transfer curve due to creep

Figure 4 Modelling effects of creep

Creep behaviour is governed by three parameters α, β and m. The first parameter, α, controls the stress level at which creep occurs; the higher α, the higher the stress level at which creep effect will be more pronounced. The second parameter, β, represents the rate of creep as a proportion of the current 'elastic' displacement $(w_c - w_o)$ The third parameter, m, controls the manner in which creep decays at large times, or, for the present formulation, after a large number of increments.

Singh and Mitchell (1968) quote the following values as typical for may soils:

β (equivalent to A) ~ 0.001 - 0.1
α ~ 6-10
m ~ 0.75-1

In the examples discussed below, α and β have been varied with m taken constant at m = 1. This corresponds to a logarithmic creep law, where w increases linearly with the logarithm of time.

APPLICATION TO TENSION PILES IN CLAY

The proposed model was used to analyse the behaviour of two piles in clay tested incrementally up to failure in tension. Both were closed ended steel pipe piles 203 mm diameter and 6.4 mm wall thickness driven 9.5 m into a stiff over-consolidated clay.

Soil properties are summarised on Figure 5. The soil consists of a stiff overconsolidated boulder clay presenting an undrained strength around 120 kPa and plasticity indexes ranging from 12 to 20%. Cone penetrometer tests and sample boreholes indicated the presence of sandy layers at depths of about 2 m and at 10 to 12 m. The shear modulus G was determined by deep plate tests and self boring pressuremeter tests. Mean values were found to be around 20 MPa.

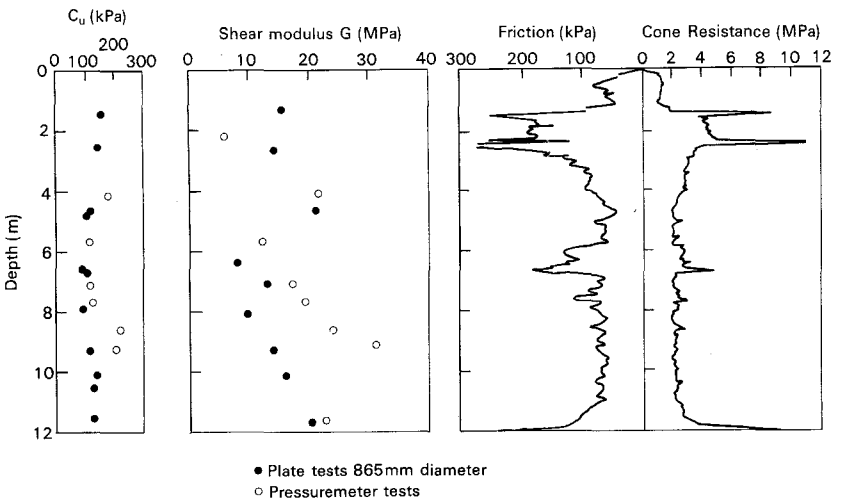

Figure 5 Soil Properties at the test site

Pile I was tested in an incremental sustained tensile loading pattern. Increments of 40 kN were applied and the resulting upward displacements were recorded during a period which varied from 1 to 12 days, as indicated on Figure 6. Failure was observed when the pull out load reached 280 kN.

On pile II a series of constant rate of loading (CRL) tests in tension and constant rate of extraction (CRE) tests were

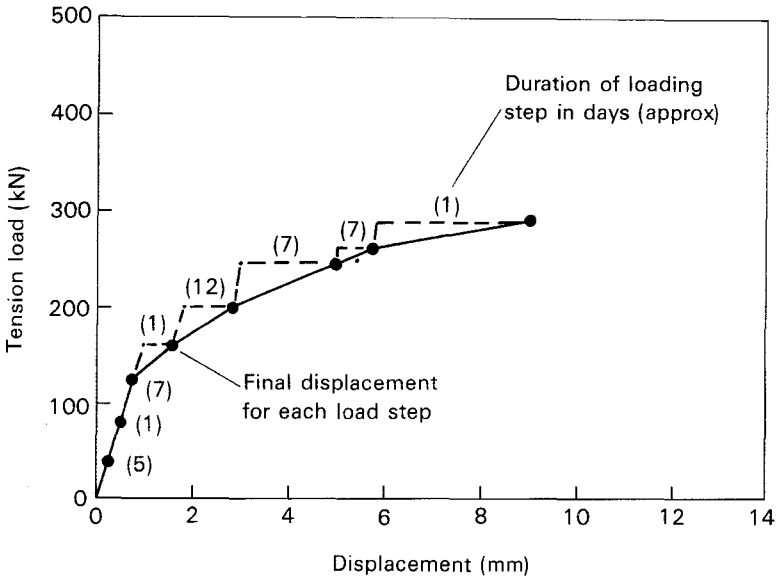

Figure 6 Test Results of Pile I

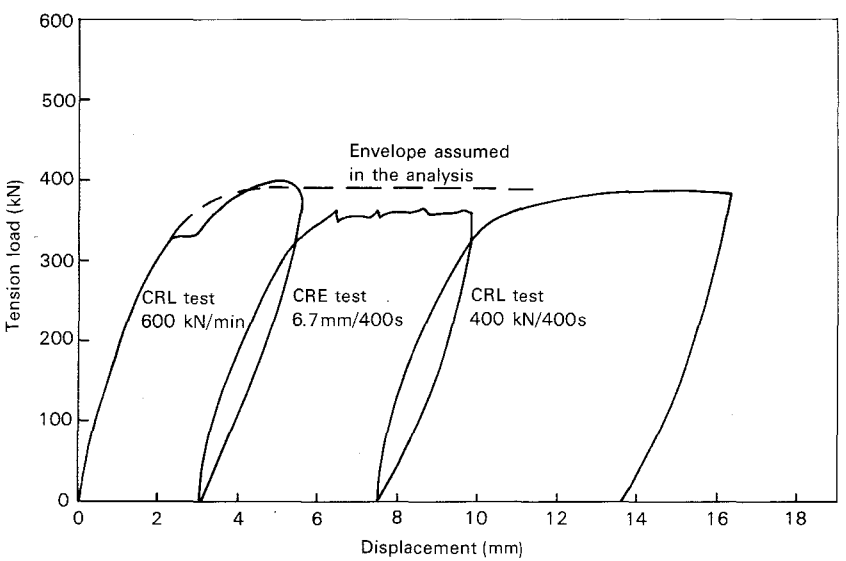

Figure 7 Test Results of Pile II

applied. The first three tests on this pile are portrayed on Figure 7, the rate of loading or extraction being indicated. Between each cycle there was a rest period which varied from

one to several days. The first failure took place around 400 kN of tension load, only 40 seconds after the start of the test. For the analysis of this test, an overall envelope was assumed and the peak load assumed to be 390 kN. Subsequent tests on this pile caused a considerable amount of degradation which will be mentioned later in this paper.

The analyses of these data consisted of: (i) evaluating the capability of the model for predicting the load settlement behaviour of those piles; and, (ii) assessing the soil parameters which lead to the best fit to the observed data.

The first study was carried out on the results of pile II tested quickly. The rate of testing on this pile was considered as standard and no effect of creep was allowed.

The following soil data was used in the program run for pile II:

Table 1
Initial Soil Parameters for Pile II (no creep assumed)

Peak skin friction	τ_{peak} = 62 kPa
Residual skin friction	$\tau_{res} = 0.6\ \tau_{peak}$
Yield skin friction	$\tau_{y} = 0.5\ \tau_{peak}$
Additional displacement that causes τ_f to reach residual	100 mm
k = 0.25 G (G = 20 000 kPa)	5000 kPa
Degradation parameter ζ	1.2

The above value of τ_{peak} was found by dividing the maximum mobilised tension load by the surface area of the pile. No allowance was made for variation of τ_{peak} with depth. Essentially this assumption followed the simple approach of assuming a peak shear stress proportional to the undrained shear strength, C_u, which was reasonably constant with depth.

Only a small adjustment, of the τ_{peak} value due to strain compatibility, was necessary to match the predicted maximum tension load to the observed value. The final τ_{peak} was 65 kPa which means that, for design C_u equal to 120 kPa, an α value of 0.54 is deduced. This agrees with the recommendations prescribed by API for stiff clays.

The first predicted pile results are shown in Figure 8. In addition, the effect of varying k was studied to match measured data on pile I. The back-figured value of k was 40% less than the initial value assumed, implying a shear modulus of G = 12 MPa. This value reflects more those from plate loading tests in Figure 5, but is lower than those from the pressuremeter tests obtained from unload reload loops.

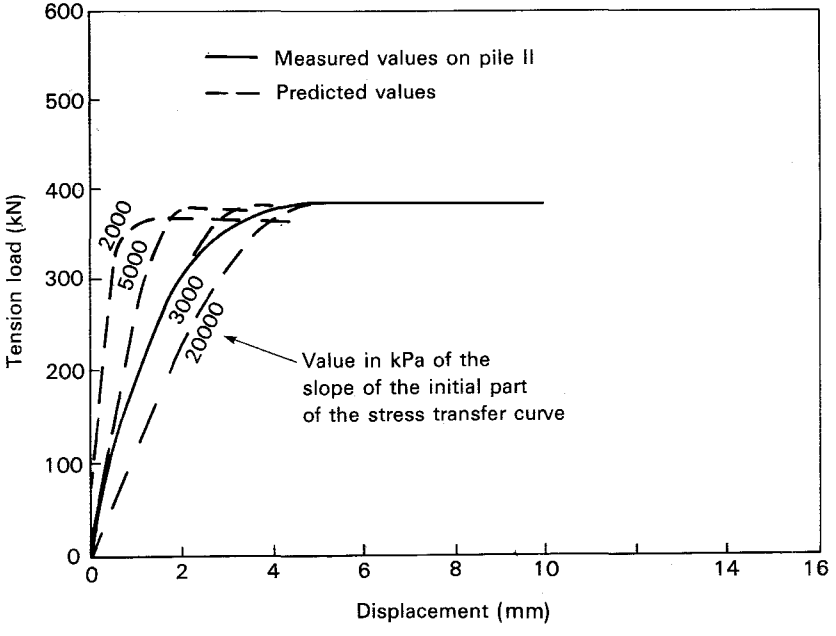

Figure 8 Fitting Predictions to the Results of Pile II

The effect of the non-linearity in the initial part of the curve was investigated by varying the value of the yield stress from nil up to 50% the of τ_{peak} shear stress, this latter value being considered an upper limit to τ_y. The results have shown very little effect of this parameter.

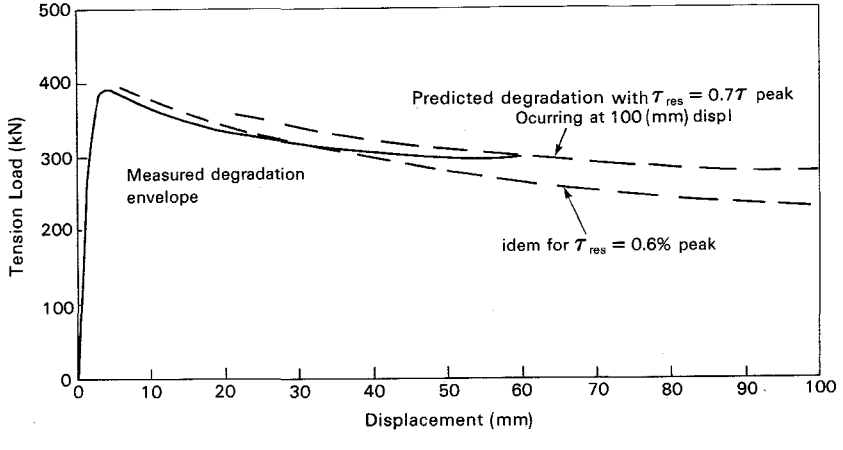

Figure 9 Comparison between measured and predicted load degradation on Pile II

A further parametric study was performed on the degradation of maximum mobilised shear stress on pile II. Figure 9 shows the measured degradation envelope compared to the forecast. The agreement is reasonably good. However pile II was tested with many loading cycles which might have influenced the amount of degradation. Degradation under cyclic loading was not modelled in the present study.

TIME EFFECTS

The difference in the peak behaviour of piles I and II, summarised below, demonstrate the effect of rate of testing.

Table 2
Summary of Measurements of Trial Tension Piles

Pile	Peak load kN	Time to failure	Peak load ratio
I	280	41 days	1.00
II	390	1 min	1.39

The difference in the behaviour can be regarded as due to:

(i) consolidation;
(ii) viscous component in soil behaviour (rate effects);
(iii) soil creep.

It is reasonable to assume the behaviour of pile I to be drained whereas pile II to be undrained.

The remaining possible causes (ii) and (iii), may be difficult to separate completely due to the large span of time to failure of the tested piles. Pore-pressure build up, which may be the principle cause of the viscous component of soil behaviour, may have influenced pile II, whereas on pile I soil creep may have been the principle cause. The boundary condition between creep and rate effects would occur for a pile tested at the maximum rate of deformation at which pore pressure variation is small.

In a recent study on strain rate effects on pile capacity, a survey by Bea (1982) quoted a 10 to 20% increase in pile capacity per log cycle of strain rate. The corresponding difference between piles I and II was found to be lower and around 6% per log cycle of time to failure. In this case the rate effects due to rapid loading were smaller than those quoted above.

Considering the points above, creep was assumed to be the predominant effect controlling the difference between the behaviour of these tested piles. Further analyses concentrate on assessing creep parameters for the soil where

the piles were installed, and evaluating the sensitivity of the results to those soil parameters.

ANALYSIS OF CREEP

Evidence from pile test data shown in the Appendix has led to the assumption that the creep parameter m is equal to 1. The different behaviour of piles I and II would then be explained by choosing the appropriate values for the remaining creep parameters α and β.

The value of α was varied from 3 to 70 to evaluate its effect on the results. Figures 10 to 13 summarise the results of the analyses and show that:

(i) for each value of α it was possible to find a corresponding β which produced a drop in the peak load prediction from pile II (quick tested, no creep assumed) to pile I (slow tested), as shown on Figure 10;

(ii) since α controls the stress level in which creep takes place, a very high α value as shown on Figure 11 will shift the creep effect to a high stress level. The analyses have shown that the values of α which led to a curve shape similar to pile I were the order of 7 to 9;

(iii) with α set to 7 the value of β was found to be 0.03 in order to produce a curve close to pile I data, as shown on Figures 12 and 13.

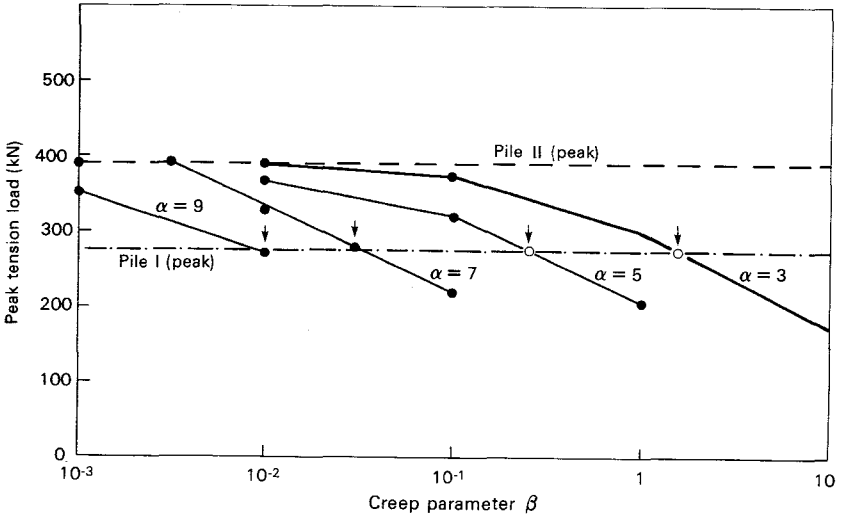

Figure 10 Influence of the creep parameters α and β on the calculated peak load

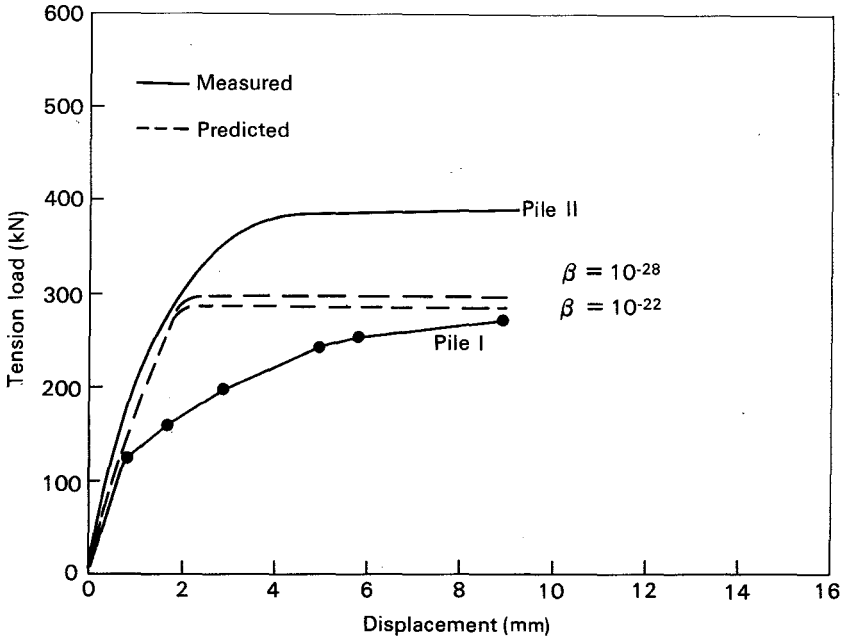

Figure 11 Comparison between measurements and predictions with $\alpha = 70$

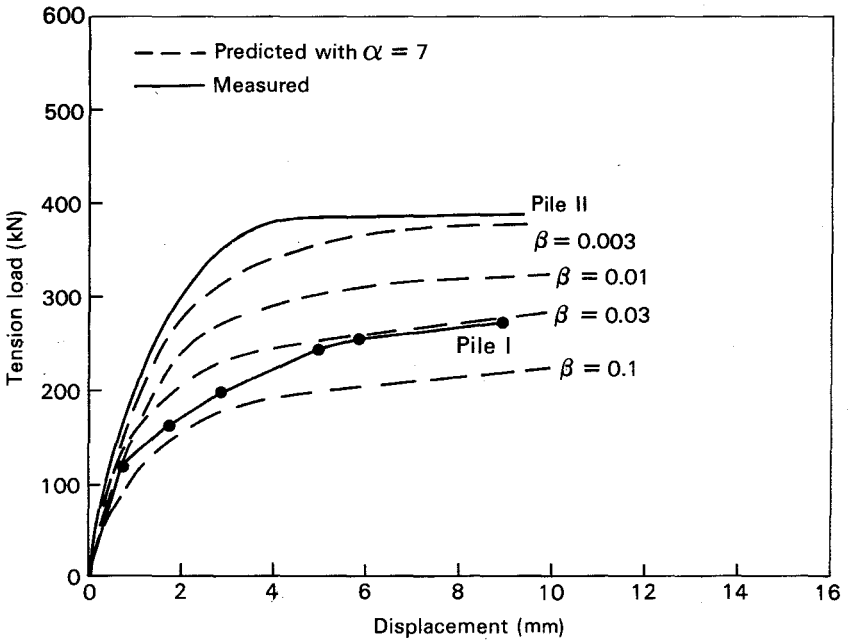

Figure 12 Effect of the parameter β

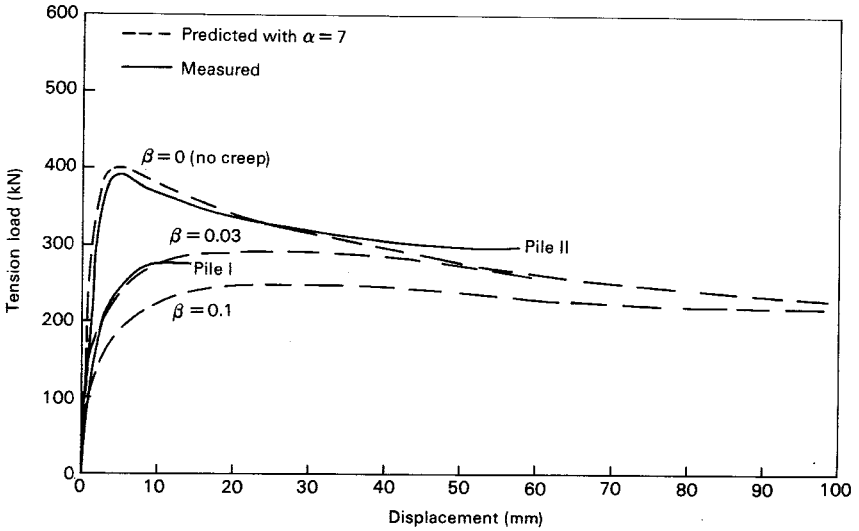

Figure 13 Assessing creep parameters

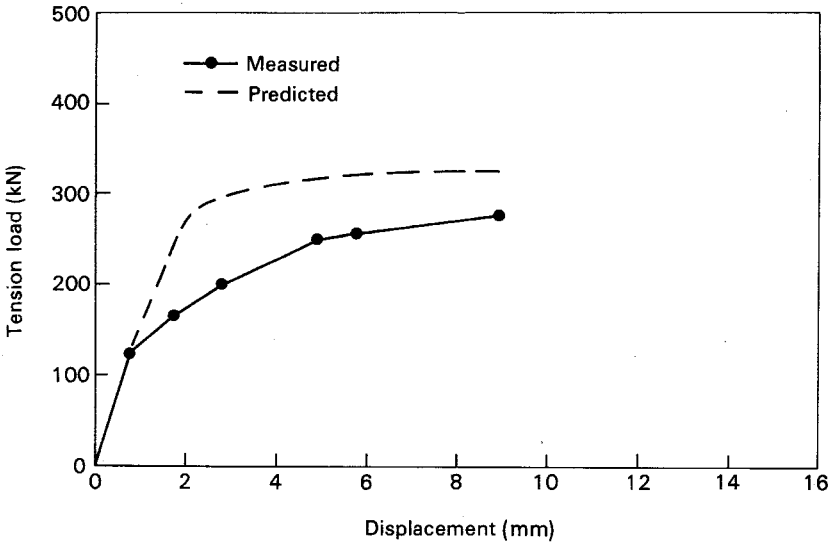

Figure 14 Comparison between measured values of Pile I and predicted values with creep parameters backfigured from field observations of displacement rate versus time

A completely different procedure was attempted for the backfiguring of creep parameters directly from the measurements of the rate of displacement of pile I, as

outlined in the Appendix. From these calculations, the following parameters were backfigured:-

$$\alpha = 13 \qquad \beta = 6 \times 10^{-5} \qquad m = 1$$

These values are different from those obtained through the computer analysis. The higher value of α may be due to the high stress level chosen for evaluating these parameters. However, applying these creep parameter values to the results of pile II, in order to simulate creep on pile I, a fair agreement is obtained. (See Figure 14.) This procedure yielded a value of peak tension load around 320 kN, whereas the measured value was 280 kN.

CONCLUSIONS

As an attempt to develop a design tool for modelling tension loaded piles, this paper has shown the use of a stress transfer curve between pile and soil interface incorporating creep. In applying this method to analyse the behaviour of two piles, tested in tension with very different times to reach failure, the following main conclusions were reached:

1 Backfigured values of soil stiffness were slightly lower than values deduced from field tests.

2 Degradation of maximum mobilized tension load due to cycling from peak to zero load on pile II, was matched with the model by considering that a residual shear stress equal to 60% to 70% of peak stress was reached after a displacement of 100 mm after peak.

3 The evaluation of soil creep parameters from the difference in the behaviour of piles I and II yielded the following values:-

$$m = 1 \qquad \alpha = 7 \qquad \beta = 0.03$$

Those values fall in the range suggested by Singh and Mitchell (1968).

4 A curve fitting technique was used for backfiguring creep parameters directly from the measurements of displacement rate versus time on piles. The backfigured values were different from those above, perhaps due to the stress levels in the pile test chosen for this analysis. However, the application of those parameters in the described model to explain the difference in the behaviour of two piles, yielded a value of peak load for pile I of 320 kN, close to the measured value of 280 kN.

ACKNOWLEDGMENTS

The support of CNPq, the Brazilian National Research Council, allowed the first author to carry out post doctoral studies on offshore geotechnics in Britain as an attached worker at the Building Research Station. Their support and facilities provided are acknowledged.

REFERENCES

API RP 2A (1980) Recommended Practice for Planning, Designing and Constructing Fixed Offshore Platforms, 12th Edition, Dallas, Texas, American Petroleum Production Department.

Bea, R B. (1982) Soil Strain Rate Effects on Axial pile Capacity. Proc. 2nd Conference on Numerical Methods in Offshore Piling, Univesity of Texas, Austin, pp 107-132.

Burland, J B. (1973) Shaft Friction of Piles in Clay - A Simple Fundamental Approach,. Ground Engineering, Vol 6, pp 30-42.

DNV (1981) Rules for the Design Construction and Inspection, of Offshore Structures. Det Norske Veritas, Oslo.

Gallagher, K A and St John, H D. (1978) Field Scale Model Studies of Piles as Anchorages for Buoyant Platforms. Proc 2nd European Offshore Conference, London.

Hamilton, J R and Barrack, J W. (1978) Floating Production Systems. Proc 2nd European Offshore Petroleum Conference, London, Vol 2, pp 45-58.

Kraft, L M. (1982) Effective Stress Capacity Model for Piles in Clay. Journal of the Geotechnical Engineering Division, ASCE, Vol 108, GT 11, pp 1387-1404.

Kraft, L M, Ray, R P and Kagawa, T. (1981) Theoretical T-Z Curves. Journal of the Geotechnical Engineering Division, ASCE, Vol 107, GT 11, pp 1543-1562.

Randolph, M F. (1982) The Performance of Piles in Clay under Tensile Axial Loading. Unpublished report to the Building Research Establishment.

Randolph, M F and Wroth, C P. (1978) Analysis of Deformation of Vertically Loaded Piles. Journal of Geotechnical Engineering Division, ASCE, GT 12 pp 1465 - 1488.

Randolph, M F and Wroth, C P. (1982) Recent Developments in Understanding Axial Capacity of Piles in Clay. Ground Engineering, Vol 15, No 7, pp 17-25,32.

Singh, A and Mitchell, J K. (1968) General Stress - Strain - Time Function for Soils. Journal of Soil Mechanics and Foudnation Engineering Division, ASCE, Vol 94, SM1 pp 21-46.

St John, H D. (1980) A Review of Current Practice in the Design and Installation of Piles for Offshore Structures. State of the Art Report published by CIRIA, London, 150p.

St John, H D, Randolph, M F, McAnoy, R P and Gallagher, K A. (1983) Design of Piles for Tethered Platforms. Proc. ICE Conference on Recent Developments in the Design and Construction of Offshore Structures, London.

Tetlow, J and Leece, M. (1982) Hutton TLP Mooring System. Proceedings 14th OTC, Houston, paper OTC 4428. pp 573-584.

Vijayvergiya, V N and Focht, J A. A New Way to Predict the Capacity of Piles in Clay. Proc. of 4th OTC, Houston, paper OTC 1718, pp 865-874.

APPENDIX

DEDUCING CREEP PARAMETERS FROM FIELD MEASUREMENTS OF RATE OF DISPLACEMENTS VERSUS TIME ON PILES:

Creep Models: Singh and Mitchell's

$$\Delta w = A \exp(\alpha \tau_c/\tau_f) (to/t)^m \Delta t \qquad \text{Equation (A1)}$$

Program's

$$\Delta w = \beta (w_c - w_o) \exp(\alpha \tau_c/\tau_f) (\Delta t/t)^m \qquad \text{Equation (A2)}$$

where

Δw = displacement increment

A, α, β, m = creep parameters

τ_c = current shear stress

τ_f = shear stress at failure

t_o = reference time

t = current time

Δt = increment of time

w_c = current displacement

w_o = displacement after rebound from τ_c to zero shear stress

Comparing equations A1 and A2:

$$\beta = \frac{A}{(w_c - w_o)} \quad \frac{t_o^m}{t^{m-1}}$$

Equation A2 was obtained by assuming the standard or reference time to to be proportional to the current shear stress τ_c or to the quantity $(w_c - w_o)$. In order to make equation A2 simpler to be applicable to field measurements, an additional assumption was made: the quantity $(w_c - w_o)$ was assumed to be proportional to the current mean shear stress on the pile surface.

This means:

$$w_c - w_o = K \tau_m \qquad \text{Equation (A4)}$$

where τ_m is the mean shear stress acting on pile soil interface

It can be written that: $\tau_m = \frac{T_c}{2\pi r_o l}$

where:

T_c = current tension load applied to the pile top

r_o = radius of the pile

l = length of the pile

Entering Randolph and Wroth's (1978) solution for an elastically loaded pile in homogeneous soil we get:

$$\frac{T_c}{w_c - w_o} = \frac{2\pi}{\zeta} \; l \; G \; \frac{\tanh(\mu l)}{\mu l}$$

where: $\zeta = \ln\left[2.5 \frac{l}{r_o} (1 - \nu)\right]$

$$\mu l = \frac{l}{r_o} \frac{2}{\zeta \lambda}$$

$$\lambda = \frac{E_{pile}}{G} \frac{2t}{r_o}$$

t = pile wall thickness

G = shear modulus of the soil

ν = Poisson's ratio of soil

E_{pile} = Young's modulus of pile material

It can be shown that:

$$K = \frac{\zeta \, r_o \, \mu l}{G \tanh(\mu l)} \qquad \text{Equation (A5)}$$

Note: ζ is a different parameter than the degradation parameter occurring in the main text.

Using equations A5 and A4, equation A2 can be rewritten, allowing $\tau_c = \tau_m$:

$$\Delta w = \beta \exp(\alpha \, \tau_c / \tau_f) \, K \tau_m \, (\Delta t / t)^m \qquad \text{Equation (A6)}$$

Assuming $m = 1$, creep parameters α, β can be obtained from plots of log $\dot{w}$ versus log t:

$$\log \dot{w} = \log \beta K \tau_m + \alpha \, \tau_m / \tau_f \log e - m \log t \qquad \text{Equation (A7)}$$

At a time $t^* = t$, for two different load levels, it comes from equation A7:

$$\log \dot{w}_1 - \log \dot{w}_2 = \log K\tau_{m1} - \log K\tau_{m2} + \alpha \frac{\tau_{m2} - \tau_{m1}}{\tau_f} \log e$$

$$\therefore \quad \alpha = \frac{\tau_f}{\tau_{m2} - \tau_{m1}} \ln \frac{\dot{w}_1/\dot{w}_2}{\tau_{m1} \quad \tau_{m2}} \qquad \text{Equation (A8)}$$

A value of β can be eventually obtained from equation A6, which rearranged is:

$$\beta = \frac{\dot{w}t}{K\tau_m \exp(\alpha \tau_c/\tau_f)} \qquad \text{Equation (A9)}$$

EXAMPLE OF CALCULATION OF CREEP PARAMETERS FROM MEASUREMENTS ON PILE I:

(1) Determining the value of K (Eq.A5):

Setting $r_o = 0.101$ m
$t^o = 0.0064$ m
$E_{pile} = 210 \times 10^6$ kPa

$G = \frac{k}{0.25} = \frac{3000}{0.25} = 12000$ kPa (k from fitting the program to pile data II)

$\nu = 0.3$

$l = 9.5$ m

We obtain: $\lambda = 2218$
$\xi = 5.10$
$\mu 1 = 1.25$

$K = 6.32 \times 10^{-5} \frac{m}{kPa}$

(2) From the plot log $\dot{w}$ versus log t (Figure A1) (considering m = 1) we have:

for load level 200 kN $\dot{w} = 10^{-3}$ mm/min for t = 100 min
for " " 240 kN $\dot{w} = 2.8 \times 10^{-3}$ " " " "

$\tau_f = 65$ kPa

$\tau_{m1} = \frac{200}{6} = 33$ kPa $\quad \tau_{m2} = \frac{240}{6} = 40$ kPa

Applying equation (A8):

$$\alpha = \frac{65}{40-33} \ln \frac{2.8 \times 10^{-2}/10^{-3}}{40-33} \simeq 13$$

(Equation A9) for t = 100 min

$$\beta = \frac{10^{-3} \times 10^{-3} \times 100}{33 \times 632 \times 10^{-3} \exp 13 \times \frac{33}{65}} = 6.5 \times 10^{-5}$$

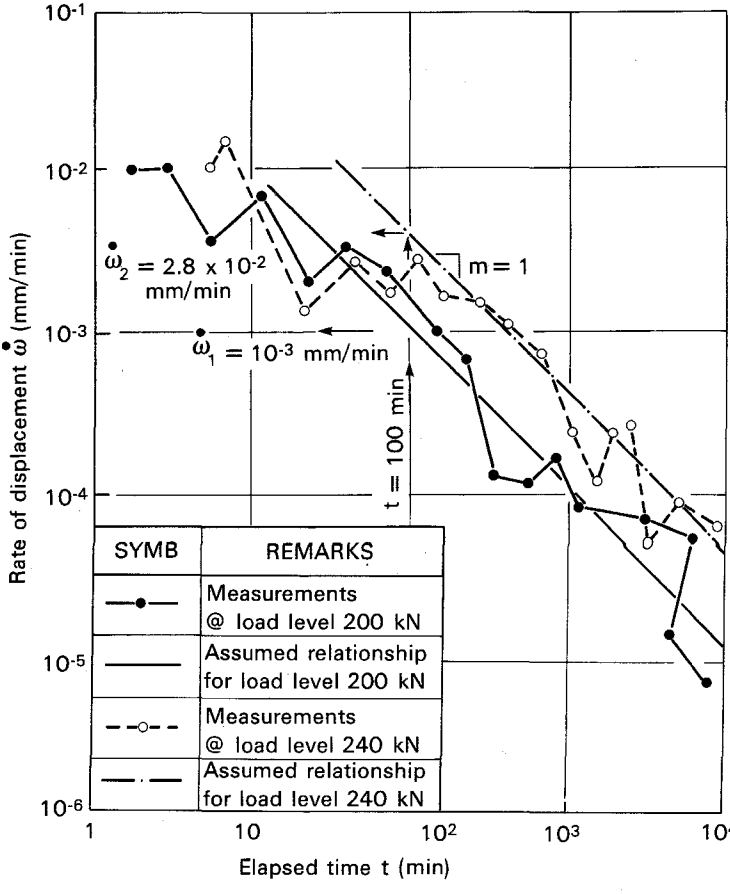

Figure A1 Evaluation of creep parameters from field measurements on Pile I